EFFECT OF FLARES ON SOLAR OSCILLATION CHARACTERISTICS

Ashok Ambastha[1], Sarbani Basu[2], and H. M. Antia[3]

[1]Udaipur Solar Observatory, Physical Research Laboratory, P. O. Box 198, Udaipur 313001, India
[1]email: ambastha@prl.ernet.in
[2]Astronomy Department, Yale University, P. O. Box 208101, New Haven CT 06520-8101, U. S. A.
[2]email: basu@astro.yale.edu
[3]Tata Institute of Fundamental Research, Homi Bhabha Road, Mumbai 400005, India
[3]email: antia@tifr.res.in

ABSTRACT

We use ring diagram analysis to study the effect of solar flares on oscillation mode characteristics, using data from GONG+ and MDI. The data taken around the flares of June 6–7, 2000; March 29, 2001 and April 10–11, 2001 are studied. We find that during some flares, the power in acoustic modes increases beyond the normal values expected from the influence of magnetic field.

Key words: Sun: oscillations; Sun: activity; Sun: interior.

1. INTRODUCTION

Solar flares are amongst the most energetic phenomena observed on the solar surface. There have been some observations (Kosovichev & Zharkova 1998, 1999) suggesting that some large flares excite waves on the solar surface. Most of the flare energy is emitted in the chromosphere and corona, however, some white light flares imply that there may still be substantial energy released in the photosphere which can affect the solar oscillations. In order to study the effect of flares on solar oscillation modes we use the ring diagram technique (Hill 1988; Patrón et al. 1997; Basu et al. 1999) applied to 3D spectra from GONG+ and MDI instruments. We use ring diagram spectra obtained before, during and after the flares to study if there is any variation in mode characteristics such as frequency, width, power and asymmetry.

2. DATA AND TECHNIQUE

To study the effect of flares, we have chosen 3 active regions which caused flares when they were close to the central meridian. These regions are NOAA9026, NOAA9393 and NOAA9415. Major flares from these regions around the time covered by our study are given in Table 1. Solar active region NOAA 9393 was the largest active region observed in the last 20 years. It produced 23 M and 5 X class flares, including the largest X20 flare of Solar Cycle 23, during its disk transit of March 24–April 5, 2001. The region was covered extensively from the Udaipur Solar Observatory (USO), India, and several of its M & X class flares were observed using USO's high resolution H_α telescope. Throughout its disk passage, solar weather remained unsettled due to its flare and CME activity, notably two large proton events. We have studied solar oscillation characteristics during one of the large proton flares in NOAA 9393, the X1.7/1B event on March 29, 2001/10:15 UT, which was associated with a Type IV radio sweep, a tenflare of 4700 sfu, and an earth-directed full halo CME reported from LASCO/SOHO imagery. The location of the flare N20W19 near the disk-center was favorable for our study, as compared to the other more spectacular flare of April 02, 2001/2132UT (Location: N19W74) estimated to be an X20, the largest observed so far in this solar cycle.

Table 1. Characteristics of solar Active Regions (AR) and Flares

NOAA No.	L0	Area ($10^{-6}A_\odot$)	Flare Class SXR/H_α	Location	Date	Start (UT)	End (UT)
9026	074	0820	X1.1	N21E23	06JUN00	13:30	13:46
	074	0820	X2.3	N19E14	06JUN00	14:58	15:40
	074	0800	X1.2/3B	N23E03	07JUN00	15:34	16:06
9393	151	2240	X1.7/1B	N20W19	29MAR01	09:57	10:32
9415	358	0710	X5.6/SF	S21E31	06APR01	19:10	19:31
	359	0760	X2.3/3B	S23W09	10APR01	05:06	05:42
	357	0550	X2.0/SF	S19W43	12APR01	09:39	10:49

In order to study the effect of flares on solar oscillation modes, we use the ring diagram analysis technique on data sets from GONG+ and MDI. Each of the data sets covers a region of about 16° × 16° on

Proc. SOHO 11 Symposium, 'From Solar Min to Max: Half a Solar Cycle with SOHO', Davos, Switzerland, 11-15 March 2002 (ESA SP-508, June 2002)

the Sun. The MDI data sets cover a time interval of 1664 minutes, while GONG+ data from the prototype instrument covers only 512 minutes. We have chosen the data from available sets when the active region was close to central meridian. The data sets used are listed in Table 2. This table gives the heliographic coordinates of the central point as well as the central meridian longitude at midpoint in time. It also gives a measure of average surface magnetic field in the region in the form of Magnetic Activity Index (MAI) (see Rajaguru et al. 2001 for definition). For convenience each region is identified by the serial number listed in the first column.

Table 2. Regions studied using ring diagram analysis

No.	Carr. Rot.	Lat.	Lon.	CM Lon.	Start time	End time	MAI (G)
NOAA 9026 : GONG+ data sets (June 2000)							
R1	1963	10.0S	84	89	06_14:11	07_00:07	16.8
R2	1963	19.0N	75	89	06_14:11	07_00:07	143.7
R3	1963	2.0S	108	89	06_14:11	07_00:07	12.8
R4	1963	10.0S	17	22	11_14:28	12_00:24	38.7
R5	1963	19.0N	8	22	11_14:28	12_00:24	80.1
R6	1963	2.0S	41	22	11_14:28	12_00:24	14.5
NOAA 9026 : MDI data sets (June 2000)							
R7	1963	22.5N	135	135	02_13:33	03_17:16	1.3
R8	1963	22.5N	75	105	04_19:58	05_23:41	113.1
R9	1963	22.5N	75	90	05_23:10	07_02:53	113.2
R10	1963	22.5N	75	75	07_02:23	08_06:06	104.4
R11	1963	22.5N	75	60	08_05:35	09_09:18	92.3
R12	1963	22.5N	75	45	09_08:47	10_12:30	72.1
NOAA 9393 : MDI data sets (March–April 2001)							
R13	1974	15.0N	240	270	19_09:39	20_13:22	2.0
R14	1974	15.0N	240	255	20_12:57	21_16:40	2.6
R15	1974	15.0N	240	240	21_16:16	22_19:59	2.7
R16	1974	15.0N	240	210	23_22:53	25_02:36	2.0
R17	1974	15.0N	150	195	25_02:12	26_05:55	104.0
R18	1974	15.0N	150	165	27_08:48	28_12:31	168.4
R19	1974	15.0N	150	150	28_12:07	29_15:50	184.8
R20	1974	15.0N	150	135	29_15:25	30_19:08	184.5
R21	1974	15.0N	150	120	30_18:43	31_22:26	168.5
R22	1974	15.0N	150	105	31_22:01	02_01:44	154.4
NOAA 9415 : MDI data sets (April 2001)							
R23	1974	22.5S	0	15	07_17:57	08_21:31	111.1
R24	1975	22.5S	360	360	08_21:05	10_00:48	112.1
R25	1975	22.5S	360	345	10_00:23	11_04:06	108.7
R26	1975	22.5S	360	330	11_03:40	12_07:23	97.1
R27	1975	22.5S	360	315	12_06:57	13_10:40	83.8
R28	1975	22.5S	270	270	15_16:48	16_20:31	1.4

To study the effect of flares on active regions we need to take the 3D spectra of oscillation power taken at different times, when the region is at different positions with respect to the central meridian. This necessarily introduces some projection effects in the results. In order to study the effects of projection, we also analyze a control quiet region at the same latitude around this time. These control regions are also listed in Table 2, and can be distinguished by low MAI values. Mode characteristics are known to be affected by magnetic fields in active regions (Rajaguru et al. 2001) and hence for the same Carrington rotation we also study one quiet region at the same latitude as the flare for comparison. The differences between the flare regions and the quiet regions can then be compared with the expected effects of the magnetic fields using the MAI values.

To fit the 3d spectra we use a model with asymmetric peak profiles as used by Basu & Antia (1999)

$$P(k_x,k_y,\nu) = \frac{e^{B_1}}{k^3} + \frac{e^{B_2}}{k^4} + \frac{\exp(A_0 + (k-k_0)A_1 + A_2(\frac{k_x}{k})^2 + A_3\frac{k_xk_y}{k^2})S_x}{x^2+1} \quad (1)$$

where

$$x = \frac{\nu - ck^p - U_xk_x - U_yk_y}{w_0 + w_1(k-k_0)}, \quad (2)$$

$$S_x = S^2 + (1+Sx)^2, \quad (3)$$

and the 13 parameters $A_0, A_1, A_2, A_3, c, p, U_x, U_y, w_0, w_1, S, B_1$ and B_2 are determined by fitting the spectra using a maximum likelihood approach (Anderson, Duvall & Jefferies 1990). The parameter S measures the asymmetry in the peak profile. The form of asymmetry is the same as that used by Nigam & Kosovichev (1998). The mode characteristics we are interested in are the frequency (ck^p), peak power ($\exp(A_0)$), half-width (w_0) and asymmetry parameter S.

3. RESULTS

Before studying the effect of flares we try to check if there are significant projection effects arising from the different orientations of the region under study, when the region is away from the central meridian. For this purpose we have selected a quiet region during Carrington Rotation 1974, heliographic latitude 15°, longitude 240° (regions R13, R14, R15 and R16 in Table 2). By comparing the mode characteristics between the region at central meridian and when it is 30° away from meridian on either side we find that one of these pairs show no significant difference suggesting little projection effect, while in the second pair there is some difference in power, though other characteristics are not affected. As far as we can see there is no activity in this region during this time and it is not clear if the variation in peak power has some other origin or whether it reflects random fluctuations in the peak power of these modes.

Fig. 1 shows the difference in mode characteristics in the region covered by NOAA9393 at different times. All differences are taken from the time when this region was at central meridian, which includes the time when a large flare occurred. From the MAI values it is clear that the average magnetic field has not changed much between regions R18 to R21.

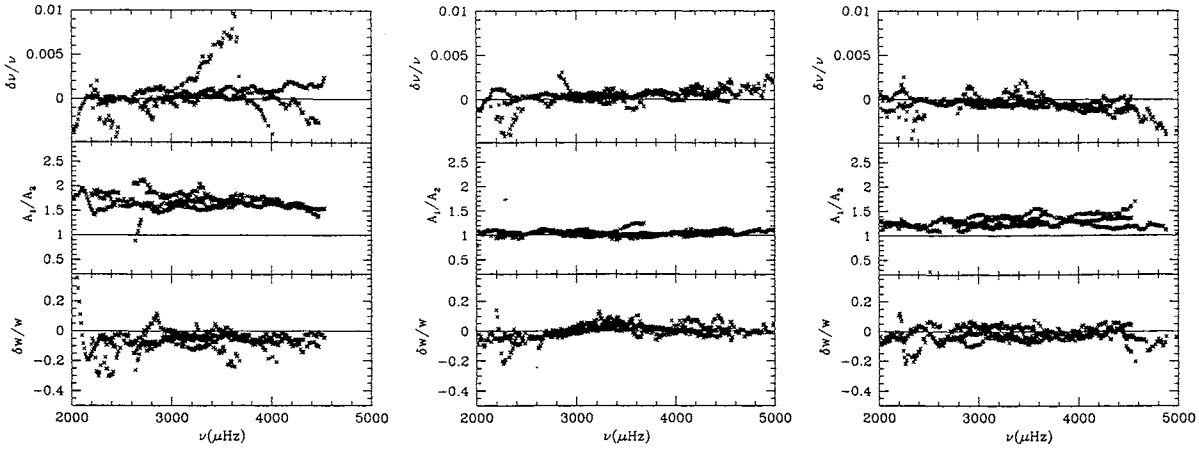

Figure 1. The relative difference in mode frequencies, and widths as well as ratio of peak power for the active region NOAA9393 when it is away from the central meridian. The left to right panels respectively, show the difference between regions $R19 - R22$, $R19 - R20$ and $R19 - R18$.

It can be seen from Fig. (1) that although region R19 has highest average magnetic field, the power in oscillations is highest amongst the regions R17–R22. This is opposite of what is expected since magnetic fields normally tend to suppress oscillations (Rajaguru et al. 2001). This suggests that the X2 flare which occurred during the observation of region R19 enhanced power in oscillatory modes. The frequencies of the acoustic modes were not significantly affected during this period, however, the small difference that is seen is of opposite sign before and after the flare This suggests some systematic changes in the magnetic field configuration, or in the structure of these layers during the flare. The frequency differences are positive for post flare spectra which may be expected from the fact that magnetic field is highest in region R19. But in the preflare spectra although the magnetic field is smaller the frequency differences have become negative, which is contrary to expectation. This could be due to complex changes taking place before the flare. Most of the change in frequency occurs in modes at high frequencies which suggests that changes are confined to outermost layers close to the photosphere. The width of the modes have not changed significantly during this period. Similarly, there is no clear difference in the asymmetry parameter S and hence that is not shown in these figures.

In order to check if similar effect is seen in other flares we look at the data from NOAA9026 which was observed by both GONG+ and MDI. In this case the flares in region R9, occurred before the active region reached the central meridian. Fig. (2) shows the difference in mode characteristics, when the region was at different locations. It includes one spectrum before the flare and one afterwards. It can be seen that between regions R9 and R8 which have very similar average magnetic field strengths, there is still some difference in power and frequencies. In region R9 when the flares took place, the power is slightly larger and the frequencies are lower; this behaviour is similar to that seen for NOAA9393. For the post flare region the variations are opposite in nature, but that is expected from the difference in magnetic field strengths. However, the magnitude of difference in width and power is much larger than what may be expected from the small difference in magnetic field. It is not clear what is the source of this additional difference. In all cases there is very little difference in frequencies during this time. Similar behaviour is seen with the GONG+ data. In this case the differences are larger than those between R9 and R10 as the magnetic field has decreased further.

We have also looked at NOAA9415 with MDI data. In this case the largest flare occurred long before the region was at the central meridian and we do not have any data before this flare. But there are two more large flares which occurred in regions R25 and R27. The magnetic field had been reducing after region R24. In this case the behaviour may be expected to be more complicated as there have been several X-class flares. Interestingly, only significant difference is found between regions R24 and R27 in power, with power being higher for region R24, which has higher magnetic field. This is contrary to what is expected from the effect of magnetic field and it is not clear if it is due to the large flare that occurred earlier. There has been a flare in region R27 also.

4. CONCLUSIONS

During some flares the power in acoustic modes appears to increase beyond the normal value expected from the influence of magnetic field. The frequencies of high degree modes appear to be reduced before some flares. This could be due to either change in structure of this region or complex magnetic field variation leading to flares. These changes should be

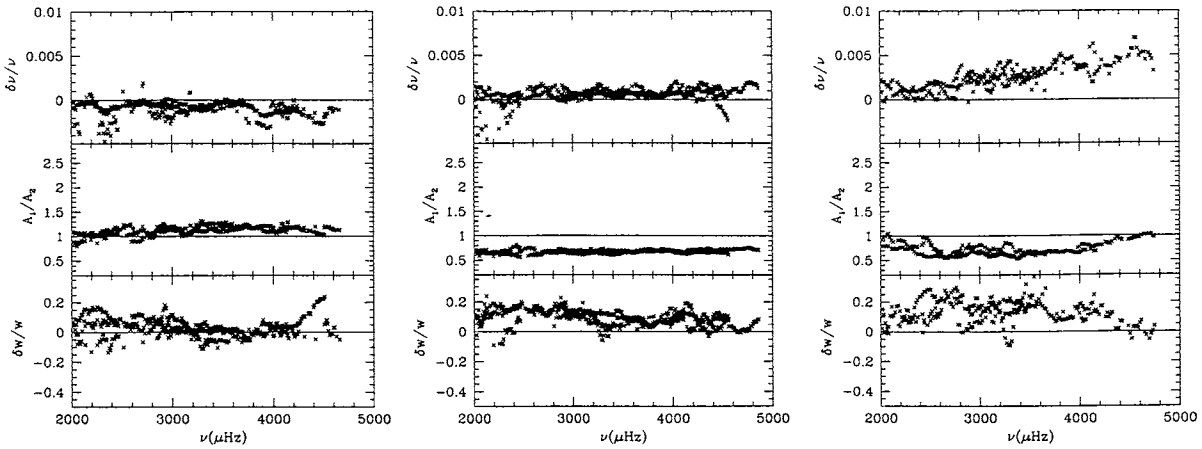

Figure 2. The relative difference in mode frequencies, and widths as well as ratio of peak power for the active region NOAA9026 when it is seen at different positions. The left to right panels respectively, show the difference between regions $R9 - R8$ (preflare), $R9 - R10$ (postflare) and $R2 - R5$ (GONG+: postflare).

confined to outermost layers around the photosphere. These signatures are not seen in all flares and there is considerable variation between different flares. Much more work is needed to understand these differences.

The observed variations in the effect of flares may perhaps be attributed to the relative amounts of deposited flare energy at the lower and deeper layers, and particularly in the photosphere. The large X-class of flare alone is not an adequate indicator of this deposition, as this parameter is related mainly to the emission from the higher, coronal level. On the other hand, a lower X-class, but higher H_α class of the flare may be more important when it comes to effects on oscillation modes. Similarly, it may be expected that the rather rare, white-light flares should excite the p-modes significantly.

ACKNOWLEDGMENTS

This work utilizes data from the Solar Oscillations Investigation/ Michelson Doppler Imager (SOI/MDI) on the Solar and Heliospheric Observatory (SOHO). SOHO is a project of international cooperation between ESA and NASA. MDI is supported by NASA grants NAG5-8878 and NAG5-10483 to Stanford University. This work also utilizes data obtained by the Global Oscillation Network Group (GONG) project, managed by the National Solar Observatory which is operated by AURA, Inc. under a cooperative agreement with the National Science Foundation. The data were acquired by the upgraded, GONG+ bread-board instrument operated at Tucson. One of us (AA) would like to thank C. Toner for providing the data. This work was supported in part by NASA Grant # NAG5-10912 to SB.

REFERENCES

Anderson, E. R., Duvall, T. L., Jr., & Jefferies, S. M. 1990, ApJ, 364, 699

Basu, S., Antia, H. M., 1999, ApJ, 525, 517

Basu, S., Antia, H. M., Tripathy, S. C., 1999, ApJ, 512, 458

Hill, F. 1988, ApJ, 333, 996

Kosovichev, A. G., Zharkova, V. V. 1998, Nature, 393, 317

Kosovichev, A. G., Zharkova, V. V. 1999, Solar Phys., 190, 459

Nigam, R., & Kosovichev, A. G. 1998, ApJ, 505, L51

Patrón, J., González Hernández, I., Chou, D.-Y., et al. 1997, ApJ, 485, 869

Rajaguru, S. P., Basu, S., Antia, H. M., 2001, ApJ, 563, 401